

A SMALL DIRECT SC AC-AC CONVERTER WITH CASCADE TOPOLOGY

KEI EGUCHI¹, FARZIN ASADI², KYOKA KUWAHARA¹, TAKA AKI ISHIBASHI³
AND ICHIROU OOTA³

¹Department of Information Electronics
Fukuoka Institute of Technology
3-30-1 Wajirohigashi, Higashi-ku, Fukuoka 811-0295, Japan
eguti@fit.ac.jp

²Mechatronics Engineering Department
Kocaeli University
Umuttepe Yerleşkesi 41380, Kocaeli, Turkey
farzin.asadi@kocaeli.edu.tr

³Department of Electronics Engineering and Computer Science
National Institute of Technology, Kumamoto College
2659-2 Suya, Koushi-shi, Kumamoto 861-1102, Japan
{ishibashi; oota-i}@kumamoto-nct.ac.jp

Received February 2018; revised June 2018

ABSTRACT. *To realize a small inductor-less AC-AC converter, this paper presents a cascade direct AC-AC converter using switched-capacitor (SC) techniques. The proposed AC-AC converter has cascade topology, where converter blocks with the conversion ratio of 1/2 or 2 are connected in series. Owing to the cascade topology, multiple conversion is performed to realize high conversion ratio. Furthermore, each converter block consists of only two capacitors and four switches, because no flying capacitor is necessary to realize AC-AC conversion. By reducing the number of capacitors, the proposed converter can achieve smaller circuit components and higher input power factor than conventional converters. To clarify the effectiveness of the proposed AC-AC converter, characteristic evaluation was performed by using simulation program with integrated circuit emphasis (SPICE) simulations and theoretical analysis. In the conversion ratio of 1/4, the SPICE simulation result demonstrated that the proposed AC-AC converter can improve 8% power efficiency and 0.4 input power factor from the conventional direct AC-AC converter using flying capacitors.*

Keywords: AC-AC converters, Cascade topology, Direct conversion, Multiple conversions, Switched-capacitor techniques

1. Introduction. In recent years, a switched-capacitor (SC) AC-AC converter is receiving much attention as an alternative appliance of autotransformers. Although the autotransformer is heavy and bulky due to magnetic core and winding, a small and light AC-AC converter can be offered by the SC techniques. The SC power converter can be designed without magnetic components [1,2]. Furthermore, the SC power converter has no core loss owing to inductor-less design. Therefore, the SC AC-AC converter can achieve higher power efficiency than the autotransformer. For this reason, several SC AC-AC converters have been proposed in the past few decades.

As far as the authors know, the first multi-level SC AC-AC converter was designed by Ueno et al. in 1993 [3,4]. By using series-parallel topology, an electroluminescent lamp

was driven by Ueno's converter. However, the first SC AC-AC converter suffers from low power efficiency. To improve power efficiency and ripple noise, Terada et al. designed the SC AC-AC converter by using ring-type converter topology [5-7]. By connecting an AC-DC converter and a DC-AC converter, the ring-type AC-AC converter can achieve not only high power efficiency but also flexible control of output waveform. However, many circuit components are necessary to design the ring-type AC-AC converter. Furthermore, the circuit control is complex, because the ring-type AC-AC converter requires multi-phase clock pulses to drive bidirectional switches. For above-mentioned reasons, the multi-level SC AC-AC converters are not effective as an alternative appliance of autotransformers.

To solve these problems, a direct SC AC-AC converter has been designed by Lazzarin et al. [8,9] and Andersen et al. [10] in 2012 and 2013. Unlike the multi-level SC AC-AC converters, an AC input is converted to the $1/2\times$ stepped-down or $2\times$ stepped-up AC voltage directly. Therefore, the number of circuit components for the direct AC-AC converter is much smaller than that for the multi-level SC AC-AC converters. Since the size of the direct SC AC-AC converter is small, it can be utilized to design not only a single-phase AC-AC converter but also a three-phase AC-AC converter [11]. However, the conversion ratio of Lazzarin's AC-AC converter is fixed to only $1/2\times$ or $2\times$. For this reason, several attempts have been undertaken to realize various conversion ratios. By expanding Lazzarin's converter, You and Hui developed the direct SC AC-AC converter realizing the conversion ratio of $1/4\times$ or $4\times$ [12]. The conventional converter topology proposed in [8-12] is the same and has flying capacitors. However, due to the flying capacitor, these converters [8-12] suffer from low power efficiency and low input power factor. Furthermore, the number of circuit components for these converters increases in proportion to the conversion ratio. Following these studies, Eguchi et al. [13,14] suggested the direct SC AC-AC converter with symmetrical topology. Owing to the symmetrical topology, Eguchi et al.'s converter [13,14] requires no flying capacitor. By reducing the number of capacitors, power efficiency and input power factor can be improved by the converter with symmetrical topology. However, the number of switches for the converter with symmetrical topology [13] is double of that for the converter with flying capacitors [8-10]. On the other hand, Do et al. developed the SC AC-AC converter by utilizing nesting voltage equalizers [15,16]. Unlike the conventional direct AC-AC converters proposed in [8-10], flexible conversion is offered by the direct SC AC-AC converter using nesting conversion. Owing to the nesting conversion, the conventional converter proposed in [15,16] can achieve higher power efficiency than the converters reported in [8-10]. However, there is still room for improvement to realize a small and efficient AC-AC converter.

In this paper, we propose a cascade direct AC-AC converter designed by using SC techniques. By cascading simple converter blocks, the proposed converter achieves high conversion ratios, such as $(1/2)^n\times$ and $2^n\times$, where n is the number of converter blocks. Furthermore, the converter block consists of only two capacitors and four switches, because the proposed converter requires no flying capacitor. In the conversion ratio of $1/2$ and 2 , the converter block can reduce one capacitor from the conventional converter proposed in [8-10]. On the other hand, the converter block can reduce 4 switches from the conventional converter proposed in [13,14]. Hence, the proposed converter will offer low-cost realization, easy production, and improve stability. Furthermore, the proposed converter can improve the characteristics, such as input power factor and power efficiency, by reducing circuit components from the conventional converters. Concerning power efficiency, input power factor, and circuit size, the effectiveness of the proposed converter is evaluated by theoretical analysis and simulation program with integrated circuit emphasis (SPICE) simulations.

The remainder of this paper is organized as follows. Section 2 presents the circuit configuration of the proposed direct converter and discusses its operation principle to emphasize the difference between the proposed AC-AC converter and existing direct AC-AC converters. Section 3 reveals the theoretical characteristics of the proposed AC-AC converter. Furthermore, theoretical comparison is performed between the proposed converter and existing converters in the point of power efficiency and hardware cost. Section 4 demonstrates the simulated characteristics, such as output voltage, power efficiency, and input power factor, in order to clarify the effectiveness of the proposed converter. Finally, the result of this work is concluded in Section 5.

2. Circuit Configuration.

2.1. Conventional AC-AC converter. Figure 1 illustrates the circuit configuration of the conventional direct SC AC-AC converters using flying capacitors [8-10,12]. The converter shown in Figure 1(a) is the simplest converter [8-10] proposed in past studies. As Figure 1(a) shows, the conventional converter consists of four bidirectional switches, S_1 and S_2 , and three capacitors, C_1 , C_2 , and C_3 , where S_1 and S_2 are driven by non-overlapped two-phase clock pulses with constant switching frequency and duty cycle. The operation principle of Figure 1(a) is as follows.

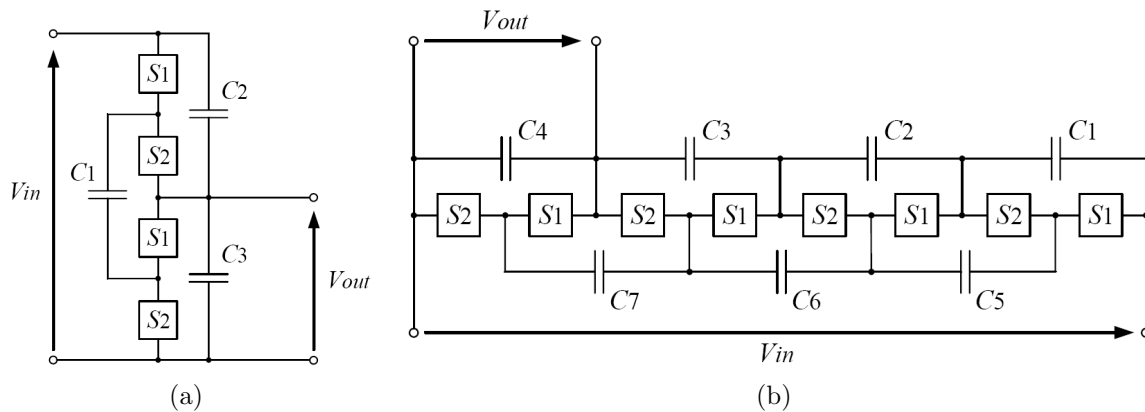


FIGURE 1. Conventional SC AC-AC converters: (a) basic converter realizing $1/2\times$ step-down conversion [8-10] and (b) expanded converter realizing $1/4\times$ step-down conversion [12]

In Figure 1(a), the AC input V_{in} and the capacitors C_2 and C_3 are connected in series. Thus, a half voltage of V_{in} is charged in C_2 and C_3 . Although only the electric charge stored in C_3 is consumed by an output load, the voltages of C_2 and C_3 are averaged by changing the connection of the flying capacitor C_1 alternately. By averaging the voltages of C_2 and C_3 , the $1/2\times$ step-down conversion is realized by Figure 1(a). Of course, by replacing the input terminal and the output terminal, the conventional converter of Figure 1(a) can generate the $2\times$ stepped-up voltage. In the case of $2\times$ step-up conversion, V_{in} is charged in C_3 . By changing the connection of the flying capacitor C_1 alternately, the voltage of C_2 becomes that of C_3 . Therefore, the $2\times$ step-up conversion is realized, because C_2 and C_3 are connected to the output terminal in series.

The output voltage of the conventional converter using flying capacitors is expressed as

$$\frac{V_{out}}{V_{in}} = \begin{cases} 1/(N + 1) & \text{(Step-down)} \\ N + 1 & \text{(Step-up)} \end{cases}, \tag{1}$$

where N is the number of stages. Furthermore, by increasing the number of stages as shown in Figure 1(b), high conversion ratio can be realized [12]. Table 1 shows the relation between the conversion ratio and the number of circuit components. As you can see from Table 1, the number of circuit components is proportional to the conversion ratio. However, the increase in the number of circuit components leads to the decrease in power efficiency and input power factor.

TABLE 1. Relation between the conversion ratio and the number of circuit components in the conventional converter

Number of stages	Conversion ratio	Number of switches	Number of capacitors
1 (Figure 1(a))	1/2	4	3
3 (Figure 1(b))	1/4	8	7
...
N	$1/(N + 1)$	$2(N + 1)$	$2N + 1$

2.2. Proposed converter. The circuit configuration of the proposed direct SC AC-AC converter is shown in Figure 2. Unlike the conventional converter of Figure 1(b), the proposed converter has cascade topology. By cascading the basic converter blocks shown in Figure 2(a), the proposed converter provides multiple conversion without flying capacitors. As Figure 2(a) shows, the basic converter block consists of four bidirectional switches, S_1 and S_2 , and two capacitors, C_1 and C_2 . Owing to the novel circuit topology, the proposed basic converter realizing $1/2 \times$ step-down conversion can achieve small and simple circuit configuration, because the proposed basic converter can reduce one capacitor from the conventional converter of Figure 1(a). Furthermore, the reduction of the

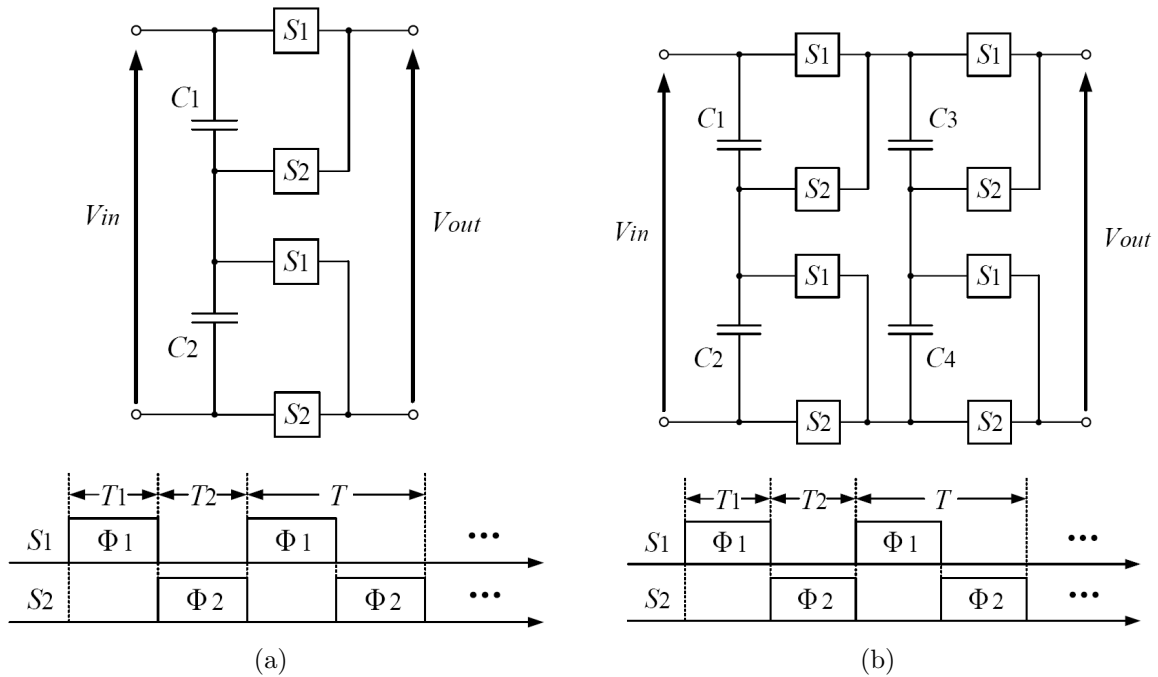


FIGURE 2. Proposed AC-AC converter: (a) basic converter realizing $1/2 \times$ step-down conversion and (b) cascaded converter realizing $1/4 \times$ step-down conversion

number of capacitors leads to the improvement of input power factor. The proposed converter is also controlled by non-overlapped two-phase clock pulses with constant switching frequency and duty cycle. The operation principle of Figure 2(a) is as follows.

In Figure 2(a), the input voltage V_{in} is divided into two by C_1 and C_2 , because V_{in} is connected to the series-connected capacitors, C_1 and C_2 . By changing the connection of the output terminal, electric charges in C_1 and C_2 are consumed equally by the output load. Therefore, the converter block of Figure 2(a) can provide the $1/2\times$ stepped-down voltage. Unlike the conventional converter of Figure 1, the proposed converter requires no flying capacitor, because the number of capacitors connected to the I/O terminals is constant. Of course, the $2\times$ step-up conversion can be realized by swapping the input/output terminals.

By cascading the converter blocks, the proposed converter generates the following output voltage:

$$\frac{V_{out}}{V_{in}} = \begin{cases} \prod_{i=1}^M \frac{1}{2} & \text{(Step-down)} \\ \prod_{i=1}^M 2 & \text{(Step-up)} \end{cases}, \quad (2)$$

where M is the number of converter blocks. Table 2 shows the relation between the conversion ratio and the number of circuit components in the proposed converter. Owing to the cascade topology without flying capacitors, the proposed converter can reduce the number of circuit components from the conventional converter. Concretely, as shown in Tables 1 and 2, three capacitors are reduced in the conversion ratio of $1/4$.

TABLE 2. Relation between the conversion ratio and the number of circuit components in the proposed converter

Number of converter blocks	Conversion ratio	Number of switches	Number of capacitors
1 (Figure 2(a))	$1/2$	4	2
2 (Figure 2(b))	$1/4$	8	4
...
M	$(1/2)^M$	$4M$	$2M$

3. Theoretical Analysis Using an Equivalent Model.

3.1. Equivalent model in the conversion ratio of $1/4$. To evaluate the properties of the proposed SC AC-AC converter, we conduct theoretical analysis by utilizing the four-terminal equivalent model [17,18] shown in Figure 3. In Figure 3, m and R_{SC} denote the turn ratio of an ideal transformer and the internal resistance of the power converter, respectively. In the theoretical analysis, the four-terminal equivalent model of the proposed converter is derived by using the instantaneous equivalent circuits of Figure 2(b). Figure 4 illustrates the instantaneous equivalent circuits of the proposed converter in the conversion ratio of $1/4$, where R_{on} is the on-resistance of the bidirectional switch, $\Delta q_{T_i, V_{in}}$ ($i = 1, 2$) is the electric charge of the input terminal in State- T_i , and $\Delta q_{T_i, V_{out}}$ ($i = 1, 2$) is the electric charge of the output terminal in State- T_i . In the four-terminal equivalent model, the parameter m is derived from the relation between the input current and the output current of Figure 4. On the other hand, the parameter R_{SC} is derived by

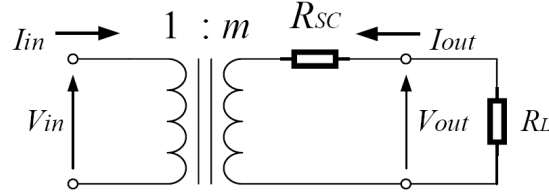


FIGURE 3. Four-terminal equivalent model

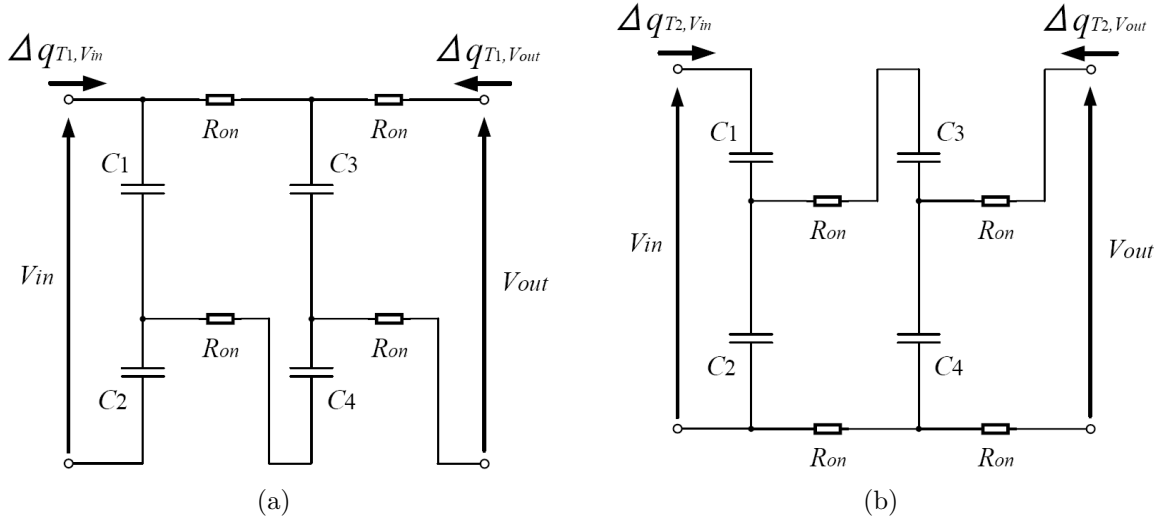


FIGURE 4. Instantaneous equivalent circuit in the conversion ratio of 1/4: (a) state- T_1 and (b) state- T_2

calculating the total consumed energy of the instantaneous equivalent circuits, where the AC input is assumed as a pulse waveform in order to simplify the theoretical analysis.

First, we discuss the differential value of electric charges $\Delta q_{T_i}^k$ in C_k ($k = 1, \dots, 4$). In a steady state, the electric charges of C_k ($k = 1, \dots, 4$) are the same at the start and end of the cycle T , because the overall change in electric charges is zero. Thus, the differential value $\Delta q_{T_i}^k$ satisfies

$$\Delta q_{T_1}^k + \Delta q_{T_2}^k = 0. \tag{3}$$

In (3), the interval of T_1 and T_2 satisfies

$$T = T_1 + T_2 \text{ and } T_1 = T_2 = \frac{T}{2}, \tag{4}$$

where T is a period of the clock pulse.

In the instantaneous equivalent circuits of Figure 4, the relation between $\Delta q_{T_i}^k$'s is obtained by using Kirchoff's current law. In Figure 4(a), the differential values of electric charges in the input and the output, $\Delta q_{T_1,V_{in}}$ and $\Delta q_{T_1,V_{out}}$, satisfy

$$\Delta q_{T_1,V_{in}} = \Delta q_{T_1}^1 + \Delta q_{T_1}^3 - \Delta q_{T_1,V_{out}}, \tag{5}$$

$$\Delta q_{T_1}^1 = \Delta q_{T_1}^2 - \Delta q_{T_1}^4, \tag{6}$$

and

$$\Delta q_{T_1,V_{out}} = \Delta q_{T_1}^3 - \Delta q_{T_1}^4. \tag{7}$$

On the other hand, in Figure 4(b), the differential values of electric charges in the input and the output, $\Delta q_{T_2,V_{in}}$ and $\Delta q_{T_2,V_{out}}$, satisfy

$$\Delta q_{T_2,V_{in}} = \Delta q_{T_2}^1, \tag{8}$$

$$\Delta q_{T_2}^1 = \Delta q_{T_2}^2 + \Delta q_{T_2}^3, \tag{9}$$

and

$$\Delta q_{T_2, V_{out}} = \Delta q_{T_2}^4 - \Delta q_{T_2}^3. \tag{10}$$

From (5)-(10), the average currents of the input/output terminals, I_{in} and I_{out} , are expressed by the overall change in electric charges. Using $\Delta q_{T_i, V_{in}}$ and $\Delta q_{T_i, V_{out}}$ ($i = 1, 2$), we have I_{in} and I_{out} as

$$I_{in} = \frac{\Delta q_{V_{in}}}{T} = \frac{\Delta q_{T_1, V_{in}} + \Delta q_{T_2, V_{in}}}{T}, \tag{11}$$

and

$$I_{out} = \frac{\Delta q_{V_{out}}}{T} = \frac{\Delta q_{T_1, V_{out}} + \Delta q_{T_2, V_{out}}}{T}. \tag{12}$$

In (11) and (12), $\Delta q_{V_{in}}$ and $\Delta q_{V_{out}}$ are electric charges in the input terminal and the output terminal, respectively. Substituting (3)-(10) into (11) and (12) yields the following relation between the input current and the output current:

$$I_{in} = -\frac{1}{4}I_{out}, \tag{13}$$

where

$$\Delta q_{V_{in}} = -\frac{1}{4}\Delta q_{V_{out}}. \tag{14}$$

Therefore, we have $m = 1/4$.

Next, the parameter R_{SC} is derived by considering the total consumed energy of Figure 4. From Figure 4, the consumed energy, W_{T_1} and W_{T_2} , is expressed as

$$\begin{aligned} W_{T_1} = & \left(\frac{\Delta q_{T_1}^4}{T_1}\right)^2 \times R_{on}T_1 + \left(\frac{\Delta q_{T_1, V_{in}} - \Delta q_{T_1}^1}{T_1}\right)^2 \times R_{on}T_1 \\ & + \left(\frac{\Delta q_{T_1, V_{out}}}{T_1}\right)^2 \times 2R_{on}T_1, \end{aligned} \tag{15}$$

and

$$\begin{aligned} W_{T_2} = & \left(\frac{\Delta q_{T_2}^3}{T_2}\right)^2 \times R_{on}T_2 + \left(\frac{\Delta q_{T_2, V_{in}} - \Delta q_{T_2}^2}{T_2}\right)^2 \times R_{on}T_2 \\ & + \left(\frac{\Delta q_{T_2, V_{out}}}{T_2}\right)^2 \times 2R_{on}T_2, \end{aligned} \tag{16}$$

where W_{T_1} and W_{T_2} are total consumed energy in Figures 4(a) and 4(b), respectively. Substituting (3)-(10) into (15) and (16) yields

$$W_T = W_{T_1} + W_{T_2} = \left(\frac{q_{V_{out}}}{T}\right)^2 \left(\frac{5}{2}\right) R_{on}T, \tag{17}$$

where W_T is the total consumed energy in one period. On the other hand, the total consumed energy of Figure 3 can be defined as

$$W_T \triangleq \left(\frac{q_{V_{out}}}{T}\right)^2 R_{SC}T. \tag{18}$$

Therefore, we have the internal resistance R_{SC} as $(5/2)R_{on}$. By combining $m = 1/4$ and $R_{SC} = (5/2)R_{on}$, the four-terminal equivalent model of the proposed converter is obtained as

$$\begin{bmatrix} V_{in} \\ I_{in} \end{bmatrix} = \begin{bmatrix} 4 & 0 \\ 0 & 1/4 \end{bmatrix} \begin{bmatrix} 1 & (5/2)R_{on} \\ 0 & 1 \end{bmatrix} \begin{bmatrix} V_{out} \\ -I_{out} \end{bmatrix}, \tag{19}$$

because the four-terminal model of Figure 4 can be expressed by the K-matrix. From (19), we get the maximum efficiency and the maximum output voltage as

$$\eta = \frac{R_L}{R_L + (5/2)R_{on}}, \quad (20)$$

and

$$V_{out} = \frac{1}{4} \left\{ \frac{R_L}{R_L + (5/2)R_{on}} \right\} \times V_{in}, \quad (21)$$

where R_L denotes the output load. As you can see from (2) and (21), the parameter R_{SC} is one of the most important factors with the influence on the characteristics of direct SC AC-AC converters. Of course, in the conversion ratio of 4, the characteristics of the proposed converter can be analyzed by the same analysis method. The theoretical analysis in the conversion ratio of 4 will be discussed in Appendix.

3.2. Comparison. Table 3 shows the comparison of the number of circuit components between the proposed converter and the conventional converters in the conversion ratio of 1/4 and 4. As Table 3 shows, the number of circuit components for the proposed converter is the smallest. Hence, the proposed converter can realize simple and small circuit configuration. Especially, the reduction in the number of capacitors leads to the improvement in power efficiency and input power factor.

TABLE 3. Comparison of the number of circuit components between the proposed converter and the conventional converters

	Conversion ratio	Number of switches	Number of capacitors
Proposed converter	1/4× or 4×	8	4
Conventional converter [8-12]	1/4× or 4×	8	7
Conventional converter [13,14]	1/4× or 4×	16	6
Conventional converter [15,16]	1/4× or 4×	8	5

Table 4 shows the comparison of characteristics concerning internal resistance, power efficiency, and output voltage. As Table 4 shows, the internal resistance R_{SC} of the conventional converter with symmetrical topology [13,14] is the smallest. Therefore, the conventional converter with symmetrical topology [13,14] achieves the highest power efficiency. On the other hand, the internal resistance of the proposed converter is the same as that of the conventional converter using nesting conversion [15,16]. In other words, the power efficiency of the proposed converter is the same as that of the conventional converter using nesting conversion [15,16].

4. Simulation. To clarify the effectiveness of the proposed converter, we conducted the characteristic comparison using the SPICE simulator. In SPICE simulations, the characteristics of the proposed converter were compared with that of the conventional direct SC AC-AC converters. The SPICE simulations were performed under conditions that $V_{in} = 220\text{V}@50\text{Hz}$, $C_1 = \dots = C_4 = 33\mu\text{F}$, $C_{out} = 1\text{nF}$, $R_{on} = 0.83\Omega$, $T = 10\mu\text{s}$, and $T_1 = T_2 = 5\mu\text{s}$, where C_{out} denotes the output capacitance of the AC-AC converter. To save space, we discuss the characteristics in the conversion ratio of 1/4 in this section.

Figure 5 demonstrates the simulated output voltage as a function of time, where the output load was set to $1\text{k}\Omega$. As you can see from Figure 5, about $55\text{V}@50\text{Hz}$ output was generated by converting the $220@50\text{Hz}$ input. As this result shows, the proposed direct

TABLE 4. Comparison of characteristics between the proposed converter and the conventional converters

	Conversion ratio	R_{SC}	Power efficiency	Output voltage
Proposed converter	1/4	$(5/2)R_{on}$	$\frac{R_L}{R_L + (5/2)R_{on}}$	$\frac{1}{4} \left\{ \frac{R_L}{R_L + (5/2)R_{on}} \right\} \times V_{in}$
	4	$40R_{on}$	$\frac{R_L}{R_L + 40R_{on}}$	$\left\{ \frac{R_L}{R_L + 40R_{on}} \right\} \times 4V_{in}$
Conventional converter [8-12]	1/4	$3R_{on}$	$\frac{R_L}{R_L + 3R_{on}}$	$\frac{1}{4} \left\{ \frac{R_L}{R_L + 3R_{on}} \right\} \times V_{in}$
	4	$48R_{on}$	$\frac{R_L}{R_L + 48R_{on}}$	$\left\{ \frac{R_L}{R_L + 48R_{on}} \right\} \times 4V_{in}$
Conventional converter [13,14]	1/4	$(3/2)R_{on}$	$\frac{R_L}{R_L + (3/2)R_{on}}$	$\frac{1}{4} \left\{ \frac{R_L}{R_L + (3/2)R_{on}} \right\} \times V_{in}$
	4	$24R_{on}$	$\frac{R_L}{R_L + 24R_{on}}$	$\left\{ \frac{R_L}{R_L + 24R_{on}} \right\} \times 4V_{in}$
Conventional converter [15,16]	1/4	$(5/2)R_{on}$	$\frac{R_L}{R_L + (5/2)R_{on}}$	$\frac{1}{4} \left\{ \frac{R_L}{R_L + (5/2)R_{on}} \right\} \times V_{in}$
	4	$40R_{on}$	$\frac{R_L}{R_L + 40R_{on}}$	$\left\{ \frac{R_L}{R_L + 40R_{on}} \right\} \times 4V_{in}$

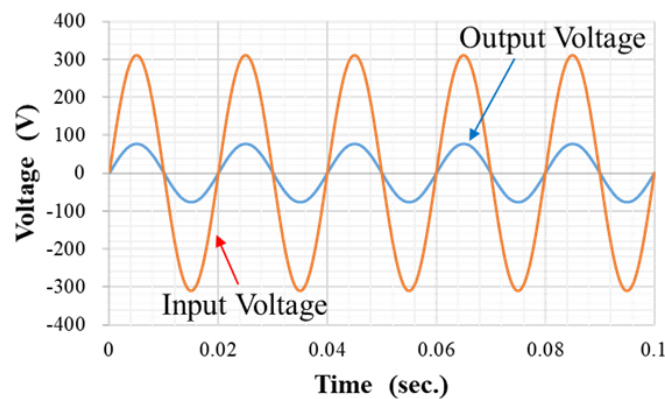


FIGURE 5. Simulated output voltage in the conversion ratio of 1/4

SC AC-AC converter can provide the $1/4 \times$ stepped-down voltage by using the multiple conversion without flying capacitors.

Figure 6 demonstrates the simulated power efficiency as a function of the output power. As Figure 6 shows, the conventional converter with symmetrical topology [13,14] achieved the highest power efficiency. On the other hand, the simulated efficiency of the proposed converter is almost the same as that of the conventional converter using nesting conversion [15,16]. These simulated results correspond to the theoretical results discussed in Section 3.2. When the output power is 0.25kW, the proposed converter improved about 8% power efficiency from the conventional converter [8-12]. Of course, the power efficiency of the AC-AC converters depends on the on-resistance R_{on} as described in Section 3.

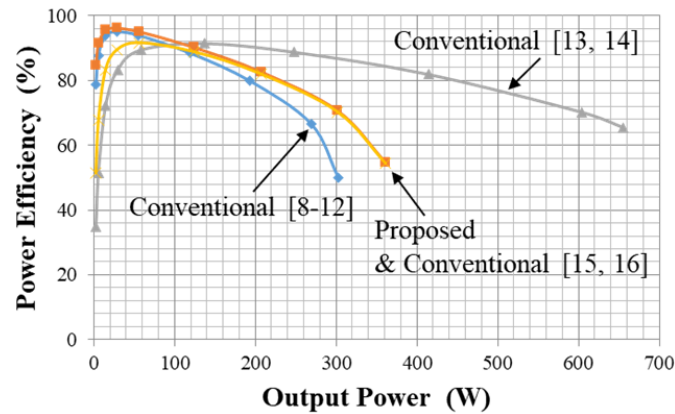


FIGURE 6. Simulated power efficiency in the conversion ratio of 1/4

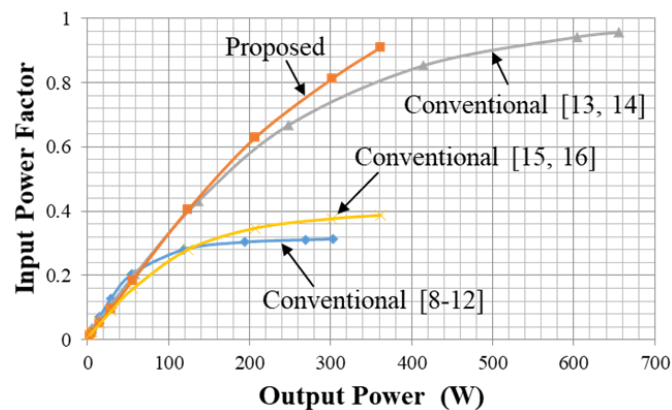


FIGURE 7. Simulated input power factor in the conversion ratio of 1/4

Figure 7 demonstrates the input power factor as a function of the output power. As Figure 7 shows, the proposed converter can realize higher input power factor than the conventional converters when the output power is more than about 150W. Concretely, when the output power is 0.25kW, the proposed converter improved more than 0.4 input power factor from the conventional converters [8-12,15,16]. The reason why the proposed converter can improve the input power factor is that the number of capacitors for the proposed converter is smaller than that for the conventional converters [8-12,15,16]. (See Table 3.) On the other hand, the input power factor of the proposed converter is almost the same as that of the conventional converter with symmetrical topology [13,14], because the number of capacitors for the proposed converter is the same as that for the conventional converter with symmetrical topology [13,14].

5. Conclusions. A small direct SC AC-AC converter with cascade topology has been proposed in this paper. Owing to the multiple conversion without flying capacitors, the proposed SC AC-AC converter provides not only small size but also high input power factor. Through SPICE simulations and theoretical analysis, the effectiveness of the proposed SC AC-AC converter was confirmed. The SPICE simulations and theoretical analysis demonstrated the following results.

Owing to the cascade topology without flying capacitors, the proposed converter can reduce the number of circuit components. Concretely, in the conversion ratio of 1/4 and 4, the proposed converter can reduce three capacitors from the conventional converter using flying capacitors. Therefore, the proposed converter can realize smaller size than

conventional converters. In the design of the direct SC AC-AC converter, this advantage will offer low-cost realization, easy production, and improve stability. Furthermore, high input power factor and high power efficiency are achieved by the reduction of circuit components. In the conversion ratio of 1/4, the SPICE simulation showed that the proposed converter improved more than 0.4 input power factor from the conventional converter using flying capacitors when the output power was 0.25kW. On the other hand, when the output power was 0.25kW, the proposed converter improved about 8% power efficiency from the conventional converter using flying capacitors. The power efficiency of the proposed converter was almost the same as that of the conventional converter using nesting conversion. From these results, we confirmed the effectiveness of the proposed converter topology.

In a future study, we are going to fabricate the laboratory prototype of the proposed SC AC-AC converter. Concerning the laboratory prototype, the experiments will be conducted to confirm the feasibility of the proposed converter.

REFERENCES

- [1] K. Abe, K. Smerpitak, S. Pongswatd, I. Oota and K. Eguchi, A step-down switched-capacitor AC-DC converter with double conversion topology, *International Journal of Innovative Computing, Information and Control*, vol.13, no.1, pp.319-330, 2017.
- [2] V. Pakala and S. Vijayan, A new DC-AC multilevel converter with reduced device count, *International Journal of Intelligent Engineering and Systems*, vol.10, no.3, pp.391-400, 2017.
- [3] F. Ueno, T. Inoue, I. Oota and I. Harada, Realization of a switched-capacitor AC-AC converter, *Proc. of the 11th European Conference on Circuit Theory and Design*, pp.1177-1180, 1993.
- [4] I. Oota, I. Harada, T. Inoue and F. Ueno, Power supply for lightening electroluminescent lamp using switched-capacitor AC-AC converter, *IEICE C-II*, vol.J77-C-II, no.12, pp.538-546, 1994.
- [5] S. Terada, I. Oota, K. Eguchi and F. Ueno, A ring type switched-capacitor (SC) programmable converter with DC or AC input/DC or AC output, *Proc. of the 2004 IEEE International Midwest Symposium on Circuits and Systems*, vol.1, pp.29-32, 2004.
- [6] S. Terada, I. Oota, K. Eguchi and F. Ueno, A switched-capacitor (SC) AC-DC or AC-AC converter with arbitrarily output voltage using the same circuit configuration, *Proc. of the 37th IEEE Power Electronics Specialists Conference*, pp.1884-1887, 2006.
- [7] K. Eguchi, I. Oota, S. Terada and T. Inoue, A design method of switched-capacitor power converters by employing a ring-type power converter, *International Journal of Innovative Computing, Information and Control*, vol.5, no.10(A), pp.2927-2938, 2009.
- [8] T. B. Lazzarin, R. L. Andersen, G. B. Martins and I. Barbi, A 600W switched-capacitor AC-AC converter for 220V/110V and 110V/220V applications, *IEEE Trans. Power Electronics*, vol.27, no.12, pp.4821-4826, 2012.
- [9] T. B. Lazzarin, M. P. Moccelini and I. Barbi, Direct buck-type AC-AC converter based on switched-capacitor, *Proc. of the 2013 Brazilian Power Electronics Conference*, pp.27-31, 2013.
- [10] R. L. Andersen, T. B. Lazzarin and I. Barbi, A 1-kW step-up/step-down switched-capacitor AC-AC converter, *IEEE Trans. Power Electronics*, vol.28, no.7, pp.3329-3340, 2013.
- [11] T. B. Lazzarin, R. L. Andersen and I. Barbi, A switched-capacitor three-phase AC-AC converter, *IEEE Trans. Industrial Electronics*, vol.62, no.2, pp.735-745, 2015.
- [12] J. You and C. Hui, A novel switched-capacitor AC-AC converter with a ratio of 1/4, *Proc. of the 2014 Int. Conf. on Electrical Machines and Systems*, pp.3205-3207, 2014.
- [13] K. Eguchi, K. Abe, I. Oota and H. Sasaki, A step-up/step-down switched-capacitor AC-AC converter with symmetrical topology, *Proc. of the 2015 International Conference on Image Processing, Electrical and Computer Engineering*, pp.14-21, 2015.
- [14] K. Eguchi, W. Do, S. Kittipanyangam, K. Abe and I. Oota, Design of a three-phase switched-capacitor AC-AC converter with symmetrical topology, *International Journal of Innovative Computing, Information and Control*, vol.12, no.5, pp.1411-1421, 2016.
- [15] W. Do, I. Oota and K. Eguchi, A switched-capacitor AC-AC converter using nested voltage equalizers, *Proc. of the 14th International Conference on Electrical Engineering/Electronics, Computer, Telecommunications and Information Technology (ECTI-CON)*, pp.314-317, 2017.

- [16] K. Eguchi, W. Do, I. Oota and H. Sasaki, Design of a step-up inductor-less AC-AC converter using nesting conversion, *ICIC Express Letters, Part B: Applications*, vol.8, no.8, pp.1191-1197, 2017.
- [17] K. Eguchi, T. Sugimura, S. Pongswatd, K. Tirasesth and H. Sasaki, Design of a multiple-input parallel SC DC-DC converter and its efficiency estimation method, *ICIC Express Letters*, vol.3, no.3(A), pp.531-536, 2009.
- [18] K. Eguchi, K. Fujimoto and H. Sasaki, A hybrid input charge-pump using micropower thermoelectric generators, *IEEJ Trans. Electrical and Electronic Engineering*, vol.7, no.4, pp.415-422, 2012.

Appendix.

A.1. Equivalent Model in the Conversion Ratio of 4. Figure 8 illustrates the instantaneous equivalent circuits of the proposed converter in the conversion ratio of 4. By using Figure 8, we derive the four-terminal equivalent model shown in Figure 3 theoretically. In Figure 8(a), the differential values of electric charges in the input and the output, $\Delta q_{T_1, V_{in}}$ and $\Delta q_{T_1, V_{out}}$, satisfy

$$\Delta q_{T_1, V_{in}} = \Delta q_{T_1}^1 - \Delta q_{T_1}^2, \quad (22)$$

$$\Delta q_{T_1}^4 = \Delta q_{T_1}^2 + \Delta q_{T_1}^3, \quad (23)$$

and

$$\Delta q_{T_1, V_{out}} = \Delta q_{T_1}^4. \quad (24)$$

On the other hand, in Figure 8(b), the differential values of electric charges in the input and the output, $\Delta q_{T_2, V_{in}}$ and $\Delta q_{T_2, V_{out}}$, satisfy

$$\Delta q_{T_2, V_{in}} = \Delta q_{T_2}^2 - \Delta q_{T_2}^1, \quad (25)$$

$$\Delta q_{T_2}^3 = \Delta q_{T_2}^1 + \Delta q_{T_2}^4, \quad (26)$$

and

$$\Delta q_{T_2, V_{out}} = \Delta q_{T_2}^3. \quad (27)$$

These equations are also obtained by using Kirchhoff's current law. Since the average input/output currents are expressed by (11) and (12), we have the following relation by substituting (22)-(27) into (11) and (12).

$$I_{in} = -4I_{out}, \quad (28)$$

where

$$\Delta q_{V_{in}} = -4\Delta q_{V_{out}}. \quad (29)$$

Therefore, the parameter m is obtained as $m = 4$.

Next, the parameter R_{SC} is derived by using the total consumed energy of Figure 8. From Figure 8, the consumed energies, W_{T_1} and W_{T_2} , are expressed as

$$\begin{aligned} W_{T_1} = & \left(\frac{\Delta q_{T_1}^2}{T_1} \right)^2 \times R_{on}T_1 + \left(\frac{\Delta q_{T_1, V_{out}} - \Delta q_{T_1}^3}{T_1} \right)^2 \times R_{on}T_1 \\ & + \left(\frac{\Delta q_{T_1, V_{in}}}{T_1} \right)^2 \times 2R_{on}T_1 \end{aligned} \quad (30)$$

and

$$\begin{aligned} W_{T_2} = & \left(\frac{\Delta q_{T_2}^1}{T_2} \right)^2 \times R_{on}T_2 + \left(\frac{\Delta q_{T_2, V_{out}} - \Delta q_{T_2}^4}{T_2} \right)^2 \times R_{on}T_2 \\ & + \left(\frac{\Delta q_{T_2, V_{in}}}{T_2} \right)^2 \times 2R_{on}T_2. \end{aligned} \quad (31)$$

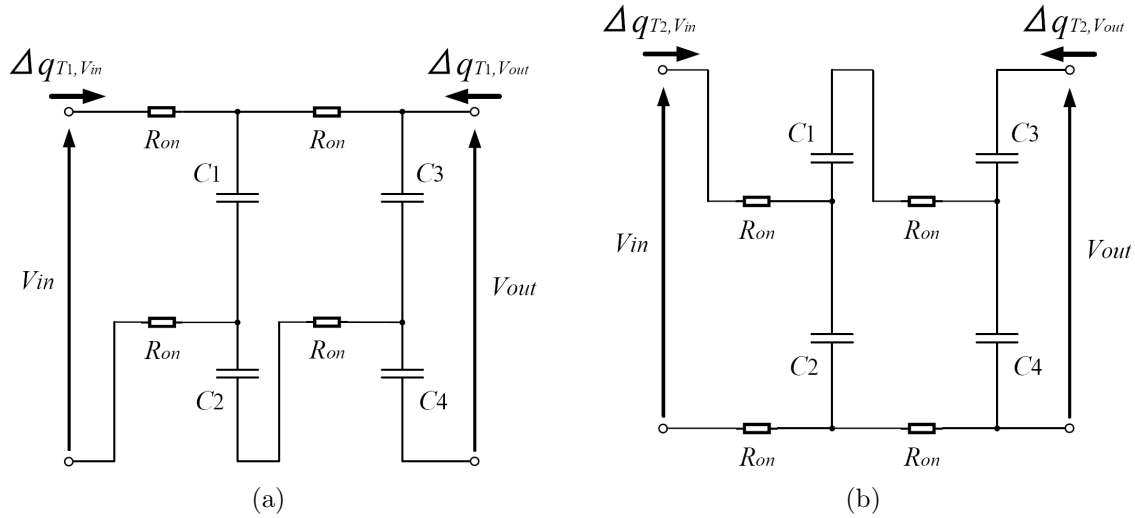


FIGURE 8. Instantaneous equivalent circuit in the conversion ratio of 4: (a) state- T_1 and (b) state- T_2

Substituting (22)-(27) into (30) and (31), the total consumed energy W_T is obtained as

$$W_T = W_{T_1} + W_{T_2} = \left(\frac{qV_{out}}{T}\right)^2 40R_{on}T. \tag{32}$$

Therefore, we get the internal resistance R_{SC} as $40R_{on}$, because the total consumed energies of the four-terminal equivalent model is expressed as (18). Finally, by combining $m = 4$ and $R_{SC} = 40R_{on}$, the four-terminal equivalent model in the conversion ratio of 4 is obtained as

$$\begin{bmatrix} V_{in} \\ I_{in} \end{bmatrix} = \begin{bmatrix} 1/4 & 0 \\ 0 & 4 \end{bmatrix} \begin{bmatrix} 1 & 40R_{on} \\ 0 & 1 \end{bmatrix} \begin{bmatrix} V_{out} \\ -I_{out} \end{bmatrix}, \tag{33}$$

because the four-terminal model of Figure 8 is expressed by the K-matrix. From (33), the maximum efficiency and the maximum output voltage are derived as

$$\eta = \frac{R_L}{R_L + 40R_{on}}, \tag{34}$$

and

$$V_{out} = \left\{ \frac{R_L}{R_L + 40R_{on}} \right\} \times 4V_{in}. \tag{35}$$